

Master regulators as order parameters of gene expression states

Andreas Krämer*

QIAGEN, Redwood City, CA 94063

(Dated: November 13, 2020)

Abstract

Cell type-specific gene expression patterns are represented as memory states of a Hopfield neural network model. It is shown that order parameters of this model can be interpreted as concentrations of master transcription regulators that form concurrent positive feedback loops with a large number of downstream regulated genes. The order parameter free energy then defines an epigenetic landscape in which local minima correspond to stable cell states. The model is applied to gene expression data in the context of hematopoiesis.

arXiv:2011.06478v1 [q-bio.MN] 12 Nov 2020

* andreas.kramer@qiagen.com

I. INTRODUCTION

The distinct cell types found in multi-cellular organisms exhibit characteristic gene expression profiles that are generally viewed as being associated with stable attracting states supported by the underlying gene regulatory network [1]. It has been proposed, that the Hopfield model [2] can be used to describe these cell type-specific expression patterns in terms of memory states [3–5], however, it is not a priori clear how such a model could be realized in a biological context. It is shown here, that the Hopfield model emerges as an *effective* model from a simple mechanism involving positive feedback loops with master transcription regulators.

In biology, master regulators (MRs) are defined as transcription factors that drive cell fate decisions [6]. MRs are important in the context of cancer [7], and essential for cellular reprogramming applications [8]. In general, they regulate expression of a large number of downstream genes, and are observed to be mutually antagonistic in different cell lineages [9], which suggests that their abundance must be highly sensitive to cell type-specific gene expression patterns. This motivates the idea that MRs are involved in positive feedback loops with the expression-regulated genes which in turn leads to stable cell states. In the model proposed here, the observed antagonism between MRs emerges indirectly because these genes are regulated concurrently. Likewise, interactions between genes that will appear in the Hopfield model, arise as *effective* interactions induced by the MRs.

A concept frequently employed in the context of cell development is that of an energy-like epigenetic landscape which guides cell state changes. This concept was first introduced by Waddington [10] as a qualitative picture (“metaphor”), and is usually portrayed as a two-dimensional surface. In the approach presented here, the epigenetic landscape is the free energy as a function of the order parameters (OPs) of the Hopfield model, i.e. it is defined in a space whose dimension is the number of cell types to distinguish, and OPs measure concentrations of MRs. Local minima in this multi-dimensional landscape then represent the different cell types.

The paper is organized as follows: In Section II it is shown that the Hopfield model is equivalent to a description in terms of feedback loops involving MRs concurrently regulating expression of a large number of genes. Section III applies this model to the hematopoietic cell lineages, and constructs an approximate epigenetic landscape from published gene expression data.

II. FEEDBACK LOOPS AND THE HOPFIELD MODEL

In the following it is assumed that gene expression is binary, i.e. genes are either “on” or “off” corresponding to open or closed chromatin configurations that enable or disable transcription controlled by transcription factors. It is furthermore assumed that cell types are statistical ensembles of individual cells with slightly varying gene expression states, so fluctuations are driven by “biological” noise. The on/off-expression state of a regulated gene i is represented by a spin variable $s_i \in \{-1, 1\}$ with $i = 1, \dots, N$, governed by a distribution $P(\{s_i\}) = \frac{1}{Z} e^{-H}$, where H is a Hopfield Hamiltonian

$$H = -\frac{1}{2} \sum_{\substack{i,j \\ i \neq j}} s_i J_{ij} s_j \quad (1)$$

with Hebbian couplings

$$J_{ij} = \frac{1}{N} \sum_k \beta_k \xi_i^k \xi_j^k. \quad (2)$$

The parameters $\xi_i^k \in \{-1, 1\}$ with $k = 1, \dots, M$, represent the stored expression pattern for cell type k , and $\beta_k > 0$ are pattern-specific coefficients with values large enough so that the Hopfield model is in the retrieval phase [11]. An equivalent formulation [12] is obtained by introducing Gaussian auxiliary variables ϕ_k , and writing the partition function $Z = Z(\{\beta_k\}, \{\xi_i^k\}) = \sum_{\{s_i\}} e^{-H}$ as

$$Z = Z_0 \sum_{\{s_i\}} \int \prod_k d\phi_k \exp \left[-\frac{N}{2} \sum_k \frac{\phi_k^2}{\beta_k} + \sum_k \sum_i \phi_k \xi_i^k s_i \right] \quad (3)$$

where the prefactor is $Z_0 = \left(\frac{N}{2\pi}\right)^{M/2} \prod_k \beta_k^{-1/2} e^{-\beta_k/2}$. Integrating out the spin variables s_i leads to

$$Z = Z_0 \int \prod_k d\phi_k \exp[-NV(\{\phi_k\})] \quad (4)$$

where the effective potential $V(\{\phi_k\})$ is given by

$$V(\{\phi_k\}) = \frac{1}{2} \sum_k \frac{\phi_k^2}{\beta_k} - \frac{1}{N} \sum_i \log 2 \cosh \left(\sum_k \phi_k \xi_i^k \right), \quad (5)$$

and the auxiliary variables ϕ_k are identified as OPs of memory states k . In the mean-field approximation, ϕ_k are given by the minima of the potential V .

In the following, we will interpret the OPs ϕ_k as concentrations of MRs that form positive feedback loops with the expression-regulated genes, as is schematically shown in Fig. 1a. This is motivated by the form of the forward and backward conditional probabilities derived from the joint probability function underlying Eq. (3),

$$P(s_i | \{\phi_k\}) \sim \exp \left(s_i \sum_k \phi_k \xi_i^k \right), \quad (6)$$

and

$$P(\phi_k | \{s_i\}) \sim \exp \left[-\frac{N}{2\beta_k} \left(\phi_k - \frac{\beta_k}{N} \sum_i s_i \xi_i^k \right)^2 \right]. \quad (7)$$

Eq. (6) shows ϕ_k as fields coupling to the spin s_i . Assuming $\phi_k \geq 0$, this can be interpreted as MR k acting as an activator ($\xi_i^k > 0$) or repressor ($\xi_i^k < 0$) on gene i , i.e. pushing the gene promotor state towards “on” or “off” in the cell ensemble. Eq. (7) in turn describes the feedback of the gene expression pattern on the MR. For large N , the distribution $P(\phi_k | \{s_i\})$ is strongly peaked, so that the value of ϕ_k is essentially a simple function of the overlap of the spin configuration s_i with the pattern ξ_i^k , $\phi_k \approx \frac{\beta_k}{N} \sum_i s_i \xi_i^k$. The feedback couplings $\beta_k \xi_i^k$, where β_k measures the strength of the feedback, are proportional to the forward couplings, therefore a MR is sensitive to its own regulation pattern, and orthogonal patterns have no

effect. Note, that in both cases the probabilities factorize, i.e. given $\{s_i\}$, the OPs ϕ_k are independent random variables. Likewise, the spins s_i are independent of each other given $\{\phi_k\}$.

To be more specific, we can describe the feedback loop using first order kinetics in an idealized model,

$$\frac{d\phi_k}{dt} = R_k - \phi_k \quad (8)$$

where

$$R_k = \frac{\beta_k}{N} \sum_i s_i \xi_i^k \quad (9)$$

is the production rate of the MR controlled by the feedback mechanism, the second term in Eq. 8 describes its degradation, and the unit of time has been set to 1. These dynamics assure that in the absence of other forces the system is always driven to the equilibrium state $\phi_k^{eq} = R_k$. Since ϕ_k is interpreted as a concentration, and R_k is a production rate, it shall always be assumed that $\phi_k \geq 0$ and $R_k \geq 0$.

For large N , ensemble fluctuations of R_k can be neglected (they are of the order $O(N^{-1/2})$), and s_i can be replaced by its ensemble average $\langle s_i \rangle = \tanh(\sum_k \phi_k \xi_i^k)$ from Eq. (6). This leads to an expression of R_k as a function of $\{\phi_k\}$ alone,

$$R_k = \frac{\beta_k}{N} \sum_i \xi_i^k \tanh\left(\sum_l \phi_l \xi_i^l\right), \quad (10)$$

thus Eq. (8) becomes

$$\frac{d\phi_k}{dt} = -\beta_k \frac{\partial V}{\partial \phi_k}. \quad (11)$$

The potential $V(\{\phi_k\})$ in Eq. (5) can therefore be interpreted as an ‘‘epigenetic landscape’’ driving the dynamics of MR concentrations ϕ_k . In the following - assuming that N is large - the sum $\frac{1}{N} \sum_i$ over expressions involving the patterns ξ_i^k is replaced by a ‘‘quenched’’ expectation value $\langle\langle \cdot \rangle\rangle$ over the random variable ξ^k . It shall be noted that it is not necessary to assume that the backward couplings are strictly proportional to the forward couplings, since ξ_i^k only appears in averages over all spins. For instance, let $\tilde{\xi}_i^k = \eta_i^k \xi_i^k$, where η^k is a random variable that is sufficiently uncorrelated with ξ^k with $\langle\langle \eta^k \rangle\rangle > 0$, then $\langle\langle \tilde{\xi}^k \cdot \rangle\rangle \approx \langle\langle \eta^k \rangle\rangle \langle\langle \xi^k \cdot \rangle\rangle$, so that $\langle\langle \eta^k \rangle\rangle$ can be absorbed in the feedback strength β_k .

The second-order term in an expansion of the potential $V(\{\phi_k\})$ around $\phi_k = 0$ is given by

$$V^{(2)}(\{\phi_k\}) = \frac{1}{2} \sum_{k,l} \left(\frac{1}{\beta_k} \delta_{kl} - \langle\langle \xi^k \xi^l \rangle\rangle \right) \phi_k \phi_l. \quad (12)$$

It is seen that the state $\{\phi_k\} = (0, 0, \dots, 0)$ is stable if the feedback strengths β_k are small enough since the first term in Eq. (12) is dominating. When β_k are increased, this state becomes unstable, and the OPs ϕ_k are driven into other minima of V away from zero. In the symmetric case where the patterns ξ_i^k are orthogonal with zero mean, $\langle\langle \xi^k \xi^l \rangle\rangle = \delta_{kl}$ and $\langle\langle \xi^k \rangle\rangle = 0$, this transition happens at $\beta_k = 1$, and stable single-memory states are found to be

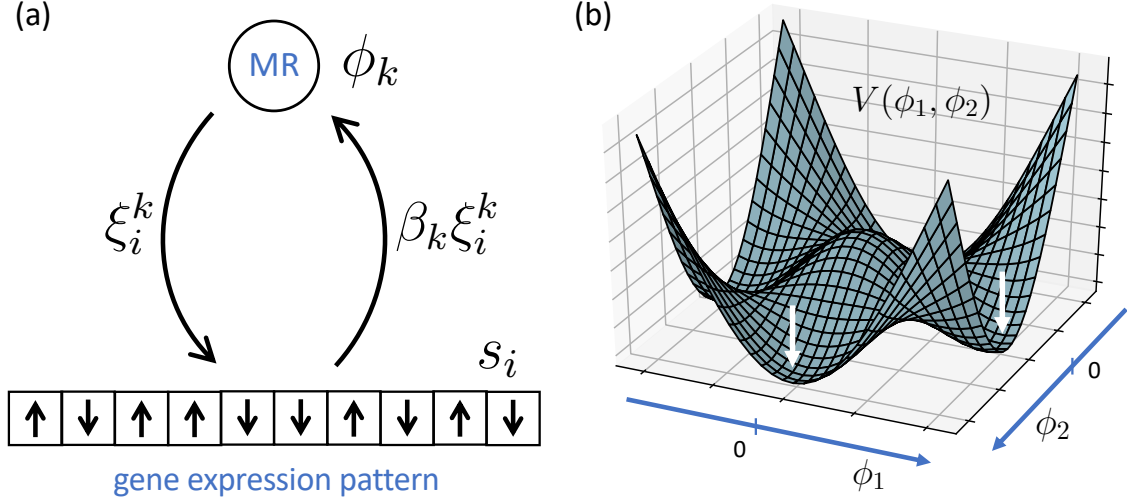


FIG. 1. (a) Positive feedback loop involving master regulator (MR) and downstream regulated genes. MR concentrations are represented by the order parameter ϕ_k , and gene expression states by the spin variables s_i . The forward and backward couplings of the feedback loop are ξ_i^k , and $\beta_k \xi_i^k$, where β_k measures the strength of the feedback. (b) The “epigenetic landscape” $V(\phi_1, \phi_2)$ for the symmetric two-dimensional case ($\beta_1 = \beta_2 = 2$). The biologically meaningful region is restricted to the positive sector $\phi_k \geq 0$ with arrows indicating the stable cell states.

of the form $\{\phi_k\} \sim (0, \dots, 0, 1, 0, \dots, 0)$. It is known that for larger values of β_k also mixtures of odd numbers of memories appear as “spurious” meta-stable states [12]. Because of the symmetry of the potential V w.r.t. sign changes of ϕ_k , in this case, the dynamics defined in Eq. (8) can be restricted to the biologically meaningful sector $\phi_k \geq 0$ (note that sign changes of ϕ_k would correspond to a flip of the corresponding spin pattern of the memory state). It then follows from Eq. (10) that the production rate R_k is also always positive or zero: $R_k = \beta_k \left\langle \left\langle \tanh \left(\sum_{l \neq k} \phi_l \xi^k \xi^l + \phi_k \right) \right\rangle \right\rangle \geq \beta_k \left\langle \left\langle \tanh \left(\sum_{l \neq k} \phi_l \xi^k \xi^l \right) \right\rangle \right\rangle = 0$, assuming mirror symmetry in the probability distribution of ξ^k . For illustration, an example of the potential V is shown in Fig. 1b for the two-dimensional case.

It shall be pointed out that several simplifying assumptions were made: The combined effect of different MRs on the expression of individual genes is assumed to be linear and additive, as is the combined effect of individual genes on MRs for the feedback. The description of the system is highly idealized since it neglects many details of gene transcription dynamics, protein translation, regulation by post-translational modification, as well as the role of co-factors and protein complexes. It is possible, that specific protein complexes may actually be key to sensing particular patterns, since their formation is sensitive to the concentration of individual protein components.

III. APPLICATION TO GENE EXPRESSION DATA

In the following, the theoretical model described above is applied to gene expression data in the context of blood cell development (hematopoiesis). Blood cells form from hematopoietic stem cells (S) in the bone marrow into different lineages of T-lymphocytes (T), B-lymphocytes (B), myeloid cells (M), and erythroid cells (E). We assume that each of these

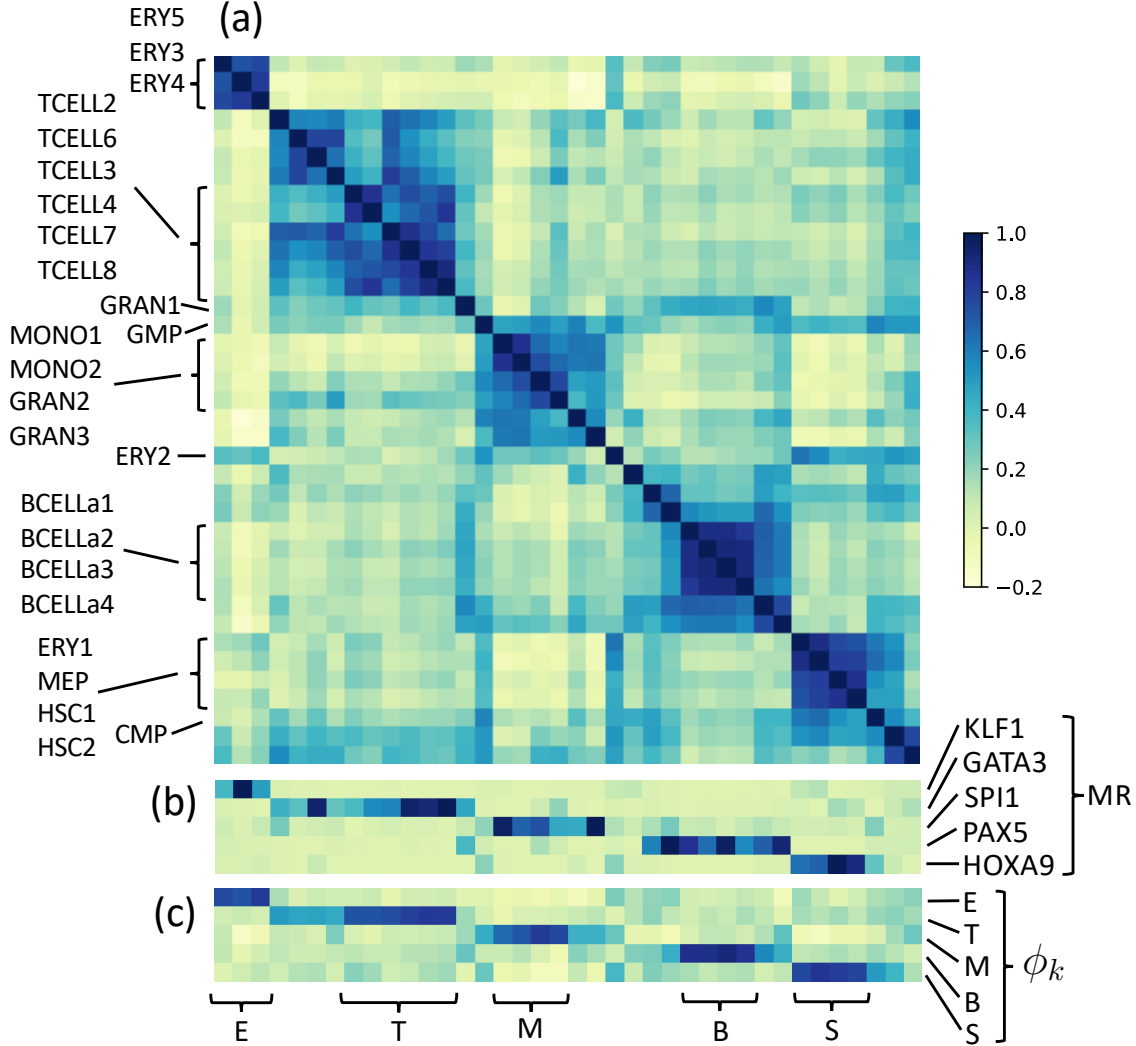


FIG. 2. (a) Cell type correlation matrix based on expression states of $N = 424$ selected genes as described in Section III.A. (b) Normalized expression for master regulators HOXA9, GATA3, PAX5, SPI1, and KLF1. (c) Corresponding computed order parameters for hematopoietic stem cell (S), T-lymphoid (T), B-lymphoid (B), myeloid (M), and erythroid (E) categories.

cell categories, rather than individual cell types, is represented by an OP ϕ_k governed by the epigenetic potential $V(\{\phi_k\})$, where $k \in \{S, T, B, M, E\}$. The view is that specific cell types are guided by the potential V , but are also subject to perturbations that depend on the detailed biology, leading to OP values close to the minima of V . If for example the effect of these perturbations is such that a (small) fraction $\frac{n}{N}$ of the spins s_i is fixed externally, i.e. not subject to regulation by $\{\phi_k\}$, then the production rate R_k , and hence the stationary state ϕ_k^{eq} is still given by the overlap of the expression pattern, $\phi_k^{eq} = \frac{\beta_k}{N} \sum_i s_i \xi_i^k$. However, as is straightforward to show, the value of ϕ_k^{eq} will be shifted due to a term added to the potential V , $\tilde{V} = \frac{n}{N} \langle \log 2 \cosh \sum_l \phi_l \xi^l \rangle - \frac{n}{N} \sum_k \gamma_k \phi_k$, where $|\gamma_k| \leq 1$.

A. Analysis

Gene expression data [13] for 38 human hematopoietic cell populations purified by flow sorting [14] was mapped onto the interval $[-1, 1]$ with -1 corresponding to “not expressed”, 1 corresponding to “expressed”, and intermediate values reflecting different levels of confidence between these two limits. This mapping is motivated by the observation that log2-scaled expression distributions for specific cell types generally exhibit a bi-modal profile with two peaks that can be interpreted as “on” and “off” gene-promoter states [15]. The map from log2-scaled gene expression values g_i to the interval $[-1, 1]$ was based on a “soft” sign function around the sample median \bar{g} , $e_i = \tanh(g_i - \bar{g})$. In total 12,953 genes were included in the analysis. The different cell populations are shown in Table I.

To apply the Hopfield model to this data, we need to first choose a meaningful set of regulated genes for which patterns ξ_i^k will be constructed. This is not a trivial task because many genes are strongly co-regulated, and others do not change their expression state across the experimental samples. The idea is to find a gene set that is minimal in some sense but maximizes information about which cell category a sample belongs to. For the analysis here, the selection of genes i was based on a heuristic that (a) controls the variance σ^2 across samples using a parameter λ , $\sigma^2(e_i) > \lambda$, and (b) subsequently maximizes independence by imposing a constraint on the Pearson correlation coefficients r controlled by a parameter μ , $\langle |r(e_i, e_j)| \rangle_{j \neq i} < \mu$, where i is fixed and the average runs over all other genes. Best parameter choices λ and μ were determined by inspecting the sample correlation matrix based on the selected gene set, and requiring optimal separation of clusters corresponding to the categories S, T, B, M, and E. For illustration, this correlation matrix is shown in Fig. 2a after hierarchical clustering for $\lambda = 0.25$ and $\mu = 0.30$. The size of the resulting set of regulated genes is $N = 424$, where the MR genes discussed below were also excluded for consistency.

TABLE I. The 38 hematopoietic cell populations from [14] for which gene expression data was analysed.

Symbol	Description
HSC1,2	hematopoietic stem cell
CMP	common myeloid progenitor
MEP	megakaryocyte/erythroid progenitor
ERY1-5	erythroid cells
MEGA1,2	megacaryocytes
GMP	granulocyte/monocyte progenitor
GRAN1-3	granulocytes/neutrophils
MONO1,2	monocytes
EOS	eosinophil
BASO	basophil
DENDa1,2	plasmacytoid and myeloid dendritic cells
Pre-BCELL2,3	B cell progenitors
BCELLa1-4	B cells
NK1-3, NKT	NK cells
TCELL1,2-8	T cells

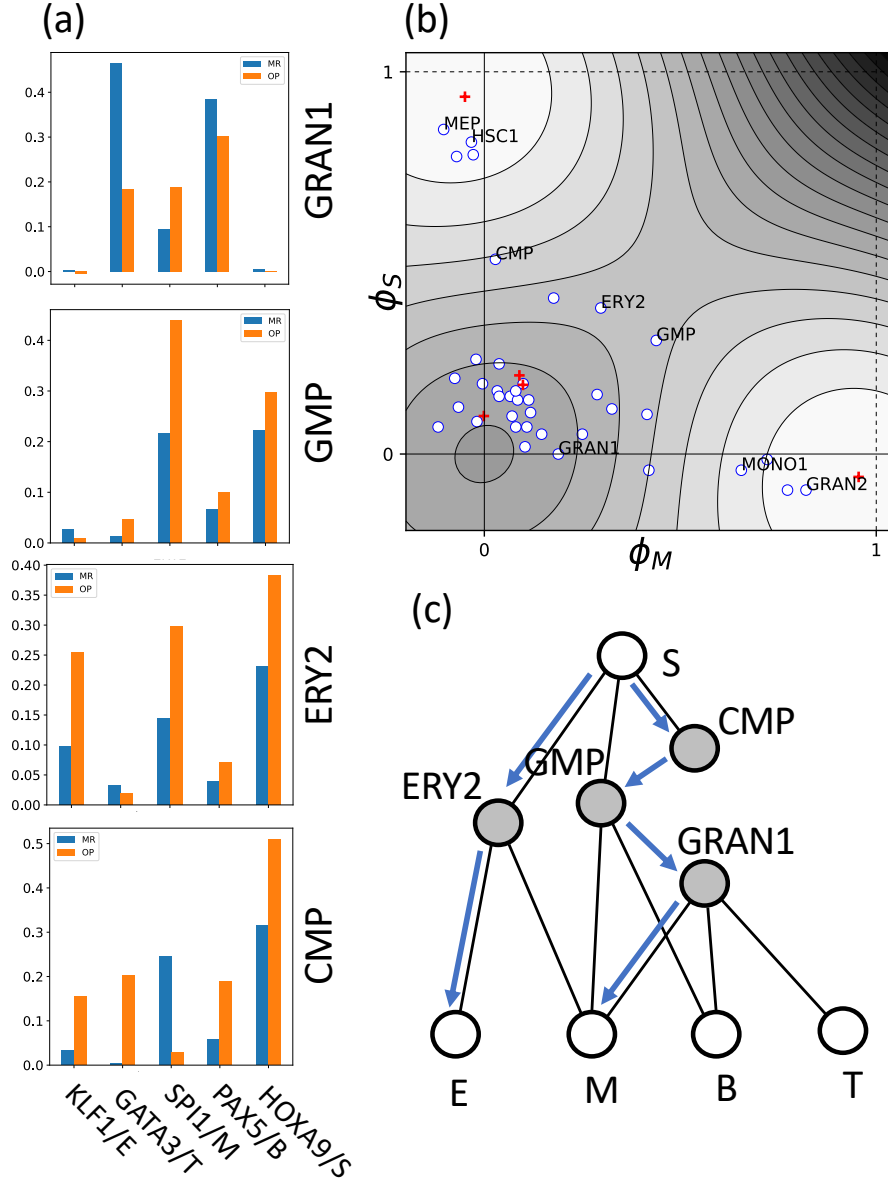


FIG. 3. (a) Comparison of order parameters and corresponding master regulators for mixed cell types GRAN1 (neutrophil progenitor), ERY2 (erythrocyte progenitor), CMP (common myeloid progenitor), and GMP (granulocyte/monocyte progenitor). (b) Cell types projected into the (ϕ_L, ϕ_S) -plane together with the potential V in that plane. Projected minima of V are shown as (+). (c) Graph illustrating the relationships of mixed cell types with the five cell categories S, T, B, M, and E. Arrows indicate the direction of development during hematopoiesis.

The cell types representing the five cell categories described above are found to be central to the clusters in Fig. 2. These are HSC1,2, MEP, ERY1 for hematopoietic stem cells, TCELL2-4,6-8 for T-lymphocytes, BCELLa1-4 for B-lymphocytes, MONO1,2, GRAN1,2 for myeloid cells, and ERY3-5 for erythroid cells. Pattern vectors ξ^k for each category $k = S, T, B, M, E$ were constructed by averaging mapped gene expression values over these cell types, and then applying the sign-function. It turns out that the resulting pattern

vectors are almost orthogonal, with values of $\langle\langle \xi^l \xi^k \rangle\rangle$, $k \neq l$, ranging from -0.057 to 0.16, and slightly biased, with values of $\langle\langle \xi^k \rangle\rangle$ between -0.32 and 0.21. The model is therefore reasonably close to the symmetric case discussed in the previous section and the condition $\phi_k \geq 0$ can be approximately fulfilled. Minima of the resulting potential $V(\{\phi_k\})$ were computed numerically. For simplicity, all parameters β_k , $k \in \{S, T, B, M, E\}$, were set to the same value β . Gradually increasing β starting from zero shows that for $\beta \gtrsim 1.5$ the point $\phi_k = 0$ becomes unstable, and for $\beta \gtrsim 2$ five minima of V exist, each with one dominating OP, and small contributions of the other OPs mixed in.

For reproducibility the source code for the complete analysis is available on github [16].

B. Results

Scaled OPs (in units of β_k), $\phi_k^{(n)} = \frac{1}{N} \sum_i s_i^{(n)} \xi_i^k$ were computed from the expression values for each cell type n , where $s_i^{(n)} = \text{sign}(e_i^{(n)})$. The results are compared to observed gene expression values (as proxy for their concentration) of known MRs for the different cell categories, HOXA9, GATA3, PAX5, SPI1, and KLF1. HOXA9 promotes hematopoietic commitment of embryonic stem cells [17], GATA3 is a MR for TH2 differentiation and controls T cell maintenance and proliferation [18], the transcription factor PAX5 is the main driver of B cell development [19, 20], SPI1 (also known as PU.1) plays a crucial role in myeloid cell development [21–23], and KLF1, as one of the core erythroid transcription factors, regulates the development of erythroid cells from progenitors [24, 25]. MR expression values (not log2 transformed) were linearly mapped to the range [0, 1]. Fig. 2 shows that both, OPs (Fig. 2c), and MR expression (Fig. 2b) correlate well with the clusters in Fig. 2a, and the cell types defining the categories S, T, B, M, and E.

Apart of cell types that are dominated by a single OP and MR, there are also intermediate types corresponding to different progenitor cells particularly for the myeloid and erythroid branches. Fig. 3a shows comparisons of MR expression and OP values for the cell types CMP (common myeloid progenitor), GMP (granulocyte/monocyte progenitor), GRAN1 (neutrophil progenitor) and ERY2 (erythrocyte progenitor). The order parameters ϕ_L and ϕ_S for these cell types are also shown in Fig. 3b, together with the potential $V(\{\phi_k\})$ in the (ϕ_L, ϕ_S) -plane. Except for CMP (which lacks an OP contribution corresponding to the myeloid MR SPI1), there is a good agreement between the observed patterns of MRs and OPs. This is graphically shown in Fig. 3c, which places those cell types in the context of the categories S, T, B, M, and E, consistent with the direction of cell development from hematopoietic stem cells to the mature cell types. A few other cell types (especially megakaryocytes and dendritic cells) do not fit well into the picture, possibly because those need to be described with additional patterns and MRs. Overall these results show that the model proposed here is consistent with gene expression data for hematopoietic cells.

IV. CONCLUSION

Biological systems involve a myriad of interacting components, and are too complicated to be understood in terms of first principles. Therefore, there is clearly a need for the development of phenomenological models abstracting from underlying biomolecular details. In this paper, I have proposed a biologically plausible model for cell type-specific states,

in which genes act collectively rather than in simple circuits through concurrent feedback loops. The model is equivalent to a Hopfield model with effective Hebbian interactions, where concentrations of master regulators are interpreted as order parameters, and an epigenetic landscape arises as their free energy. Despite its simplifying assumptions, it was shown that this model is consistent with experimental gene expression data in the context of hematopoiesis.

The model has several features that make it attractive: *Robustness*. Barriers separating stable states are of the order of the system size N [12]. Thus cell states are stable against fluctuations involving few genes. *Parallelism*. The information transmitted through the feedback loop involves many genes in parallel that are concurrently used by different regulators. This could be a prototype for intracellular communication also in other contexts since many genes are known to be shared among various cellular functions. Parallel signalling, as long as different signals are orthogonal, ensures that cross-talk is limited. *Evolvability*. The model decouples cell type-specific patterns through separate master regulators. One may therefore speculate, that evolution driving the “learning” of patterns via correlation between forward and backward regulation can occur independently for different cell types. Thus, multicellular organisms could evolve by adding more cell types without perturbing existing ones. Finally, as in the case of DNA and the genetic code for proteins, biological systems have to store information encoding their structure and function on every level. Mapping cell states onto the Hopfield model, which represents a prototypical information storage device, makes this explicit.

-
- [1] S. Huang, G. Eichler, Y. Bar-Yam, and D. Ingber, *Physical Review Letters* **94**, 1 (2005).
 - [2] J. J. Hopfield, *Proceedings of the National Academy of Sciences* **79**, 2554 (1982).
 - [3] A. H. Lang, H. Li, J. J. Collins, and P. Mehta, *PLoS Computational Biology* **10**, e1003734 (2014).
 - [4] A. T. Fard, S. Srihari, J. C. Mar, and M. A. Ragan, *npj Systems Biology and Applications* **2** (2016), 10.1038/npjbsa.2016.1.
 - [5] J. Guo and J. Zheng, *Bioinformatics* **33**, i102 (2017).
 - [6] T. L. Davis and I. Rebay, *Developmental Biology* **421**, 93 (2017).
 - [7] A. Califano and M. J. Alvarez, *Nature Reviews Cancer* **17**, 116 (2016).
 - [8] Z. D. Smith, C. Sindhu, and A. Meissner, *Nature Reviews Molecular Cell Biology* **17**, 139 (2016).
 - [9] M. Heinäniemi, M. Nykter, R. Kramer, A. Wienecke-Baldacchino, L. Sinkkonen, J. X. Zhou, R. Kreisberg, S. a. Kauffman, S. Huang, and I. Shmulevich, *Nature methods* **10**, 577 (2013).
 - [10] C. H. Waddington, *An introduction to modern genetics* (George Allen & Unwin London, 1939).
 - [11] Here we consider the slightly more general case where patterns have different weights. The parameters β_k can also be interpreted as pattern-specific inverse temperatures.
 - [12] D. Amit, H. Gutfreund, and H. Sompolinsky, *Physical Review A* (1985).
 - [13] NCBI GEO database, accession GSE24759.
 - [14] N. Novershtern, A. Subramanian, L. N. Lawton, R. H. Mak, W. N. Haining, M. E. McConkey, N. Habib, N. Yosef, C. Y. Chang, T. Shay, G. M. Frampton, A. C. B. Drake, I. Leskov, B. Nilsson, F. Preffer, D. Dombkowski, J. W. Evans, T. Liefeld, J. S. Smutko, J. Chen, N. Friedman, R. A. Young, T. R. Golub, A. Regev, and B. L. Ebert, *Cell* **144**, 296 (2011).

- [15] D. Hebenstreit, M. Fang, M. Gu, V. Charoensawan, A. van Oudenaarden, and S. A. Teichmann, *Molecular Systems Biology* **7**, 497 (2014).
- [16] <https://github.com/akraemr/hopfield-cell-state-model>
- [17] V. Ramos-Mejía, O. Navarro-Montero, V. Ayllón, C. Bueno, T. Romero, P. J. Real, and P. Menendez, *Blood* **124**, 3065 (2014).
- [18] Y. Wang, I. Misumi, A.-D. Gu, T. A. Curtis, L. Su, J. K. Whitmire, and Y. Y. Wan, *Nature Immunology* **14**, 714 (2013).
- [19] J. Medvedovic, A. Ebert, H. Tagoh, and M. Busslinger, in *Advances in Immunology*, Vol. 111 (2011) pp. 179–206.
- [20] C. Cobaleda, A. Schebesta, A. Delogu, and M. Busslinger, *Nature Immunology* **8**, 463 (2007).
- [21] P. Burda, P. Laslo, and T. Stopka, *Leukemia* **24**, 1249 (2010).
- [22] A. D. Friedman, *Oncogene* **26**, 6816 (2007).
- [23] A. Zakrzewska, C. Cui, O. W. Stockhammer, E. L. Benard, H. P. Spaink, and A. H. Meijer, *Blood* **116**, 1 (2010).
- [24] M. R. Tallack, G. W. Magor, B. Dartigues, L. Sun, S. Huang, J. M. Fitztock, S. V. Fry, E. A. Glazov, T. L. Bailey, and A. C. Perkins, *Genome Research* **22**, 2385 (2012).
- [25] P. E. Love, C. Warzecha, and L. Q. Li, *Trends in Genetics* **30**, 1 (2014).